Available online at www.sciencedirect.com
SCIENCE DIRECT®

Journal of the European Ceramic Society 24 (2004) 1725–1728

www.elsevier.com/locate/jeurceramsoc

Electron microscopy of lead and calcium pyrochlores

R. Ubic*, J.C. Merry, A.C. Leach

Department of Materials, Queen Mary and Westfield College, University of London, Mile End Road, London E1 4NS, UK

Abstract

Several compositions in the $Pb_nNb_2O_{5+n}$ system have been ascribed nearly identical distorted pyrochlore symmetries, with the degree of distortion increasing with PbO content. Rietveld refinements of neutron diffraction data for the $n=1.5$ composition have confirmed its cubic structure. Defect layers form for $n > 1.5$, and their density increases with n. The temperature coefficient of resonant frequency (TCF) of $Pb_2Nb_2O_7$ is 814 MK^{-1}. The substitution of Ta for Nb decreases TCF significantly, down to 223 MK^{-1} for $Pb_2(Nb_{0.5}Ta_{1.5})O_7$, and increases the defect density slightly. Further substitution of Ca for Pb significantly alters the structure of these defect layers, although the product remains single-phase. The structure and properties of $Ca_2Nb_2O_7$ and $Ca_2Ta_2O_7$ have also been studied. $Ca_2Nb_2O_7$ is monoclinic and ferroelectric at room temperature, containing (100) domains but no defect layers. Monoclinic $Ca_2Ta_2O_7$, on the other hand, is not ferroelectric but does contain defect layers similar in appearance to those found in Pb-niobate-tantalates.

Keywords: Defects; Dielectric properties; Electron microscopy; Niobates; Tantalates

1. Introduction

Microwave resonators are critical elements in the multi-billion dollar mobile telecommunications equipment market. Three properties are important in determining the usefulness of a ceramic material as a dielectric resonator. First, the material must have a high dielectric constant (ε_r) to enable size reduction. Second, a high quality factor Q (low tanδ) means fine frequency tunability and more channels within a given band. Third, these ceramic components play a crucial role in compensating for frequency drift because of their low temperature coefficients of resonant frequency (τ_f). Combining all these properties in a single material is not a trivial problem, and a full understanding of the crystal chemistry of such materials is paramount to future development.

It has now been well established[1–3] that the cubic form of lead pyroniobate is Pb-deficient, with only 75% of A-sites occupied ($Pb_{1.5}Nb_2O_{6.5}$). Introducing more Pb into this structure causes a rhombohedral distortion of the pyrochlore structure, the nature of which is still not completely understood. For this reason, stoichiometric $Pb_2Nb_2O_7$ does not have the cubic pyrochlore structure. Brusset et al.[4] reported a monoclinic unit cell with lattice constants $a=13.021$ Å, $b=7.483$ Å, $c=34.634$ Å, $\beta=125.18°$; however, most later work seems to suggest a trigonal structure.[1–3,5,6]

2. Procedure

Pellets with compositions in the $Pb_n(Nb_{1-x}Ta_x)_2O_{5+n}$ system were prepared by a conventional mixed-oxide route as described elsewhere.[7] Phase assemblages were checked by scanning electron microscopy (SEM, model JSM 6300, Jeol, Tokyo, Japan) and X-ray diffraction (XRD, D5000, Siemens AG, Munich, Germany) using CuK_α radiation from $10° \leqslant 2\theta \leqslant 60°$. Crystallographic parameters of the cubic $Pb_{1.5}Nb_2O_{6.5}$ phase were calculated both from XRD scans as well as neutron diffraction data ($\lambda=1.594$ Å) obtained at Institut Laue – Langevin (ILL), Grenoble, France (experiment number 5-22-568).

Some pellets underwent thinning by conventional ceramographic techniques followed by ion milling (model 600, Gatan, Pleasanton, California, USA) to electron transparency for observation in the transmission electron microscope (TEM, model JEM 2010, Jeol, Japan).

* Corresponding author. Tel.: +44-20-7882-5160; fax: +44-20-8981-9804.
E-mail address: r.ubic@qmw.ac.uk (R. Ubic).

0955-2219/$ - see front matter © 2003 Elsevier Ltd. All rights reserved.
doi:10.1016/S0955-2219(03)00482-5

Measurements of τ_f were made at Filtronic Comtek on a vector network analyser (model 8753E, Hewlett Packard, USA).

3. Results and discussion

3.1. Crystal structure

High-resolution XRD data of the cubic $Pb_{1.5}Nb_2O_{6.5}$ phase, refined by neutron diffraction scans (Fig. 1), revealed a lattice constant of 10.5622 Å and a crystallographic x parameter for the 48f oxygen positions of 0.313, in excellent agreement with previous work.[8,9] For this composition, SADPs can be indexed according to the cubic pyrochlore structure; however, for $n = 1.6$, a streaking of intensity is visible along $<111>$ directions, corresponding to the disordered stacking of defect layers in that direction shown in Fig. 2. These layers are of uniform thickness. Their main feature is that they separate and shear regions of otherwise un-defected pyrochlore. For $n > 1.6$, discreet extra reflections appear,[3,7,10] indicating that the new structure is periodic and results in a multiplication of the $\{111\}_{cubic}$ spacing.

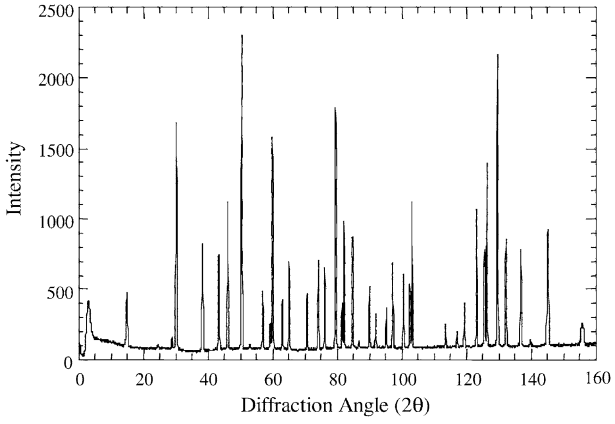

Fig. 1. Neutron diffraction data for $Pb_{1.5}Nb_2O_{6.5}$.

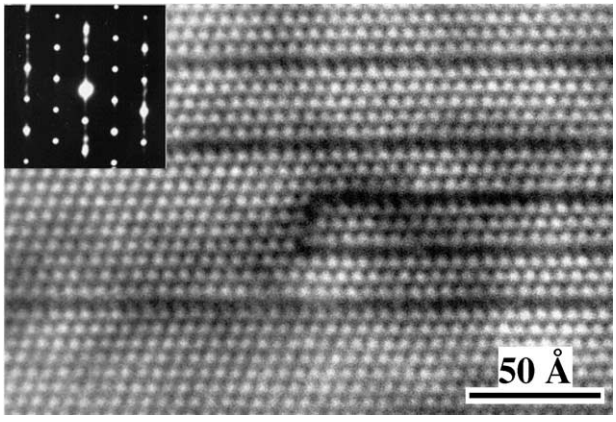

Fig. 2. High-resolution TEM image of $Pb_{1.6}Nb_2O_{6.6}$ parallel to $[110]_{cubic}$ showing its aperiodic defect structure.

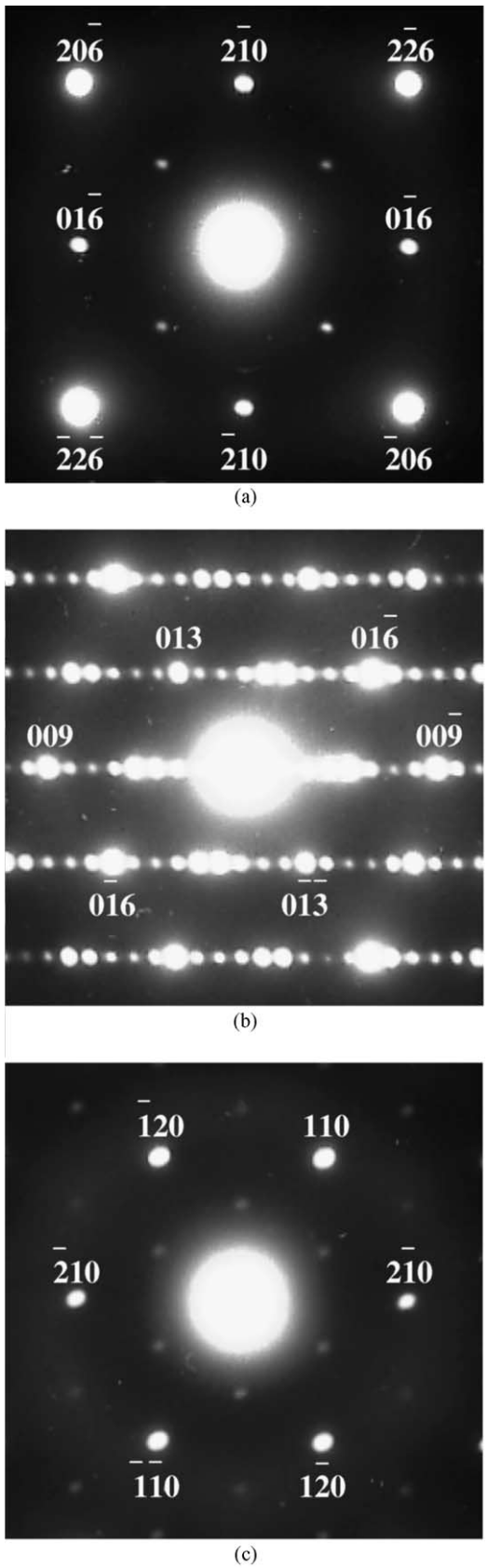

Fig. 3. Selected area electron diffraction patterns of $Pb_2Nb_2O_7$ indexed according to the trigonal unit cell as (a) [361], (b) [100], and (c) [001].

The SADP's of $Pb_2Nb_2O_7$ ($n=2$) in Fig. 3 can be indexed according to a trigonal unit cell with $a=7.436$ Å, $c=27.561$ Å. This structure is similar in appearance to the perovskite layer structure (PLS)[11] of $Sr_2Nb_2O_7$ or $Sr_2Ta_2O_7$; however, the crystallographic shear evident in Fig. 2 does not occur in PLS structures. The exact nature of these defects has yet to be determined.

Replacing some of the Nb^{+5} with Ta^{+5} has little effect on the structure; however, doping Ca^{+2} in for Pb^{+2} causes serious changes to the nature of defect layers. $Ca_2Nb_2O_7$ contains (100) ferroelectric domains at room temperature (Fig. 4) but does not show any evidence of a defect layered structure. The structure of $Ca_2Ta_2O_7$ (Fig. 5), although monoclinic,[12] is similar to that of trigonal $Pb_2(Ta_{1.5}Nb_{0.5})O_7$ in that both contain defect layers; however, whereas these defects cause crystallographic shear in the latter, no shear is evident in the former. The inset diffraction pattern in Fig. 5 can be indexed according to the monoclinic "7M" polytype reported by Grey et al.[12] Fig. 6 shows high-resolution images of $Pb_2Nb_2O_7$, $Pb_2(Nb_{0.5}Ta_{1.5})O_7$ and $(Pb_{0.6}Ca_{1.4})(Nb_{0.5}Ta_{1.5})O_7$. The structure of $Pb_2(Nb_{0.5}Ta_{1.5})O_7$ differs only slightly from $Pb_2Nb_2O_7$, having a higher density of defect layers; but the Ca-doped material is very different. Although the Ca-doped material is virtually indistinguishable from undoped ceramics by XRD (Fig. 7), this level of Ca-doping results in three fundamental changes in the nature of the defect layers. First, they are no longer of uniform thickness, but appear with two distinct thicknesses, one twice as thick as the other. Second, although occurring at a fairly high density, they are aperiodic. Third, like PLS they do not cause the crystallographic shear seen in both $Pb_2Nb_2O_7$ and $Pb_2(Nb_{0.5}Ta_{1.5})O_7$.

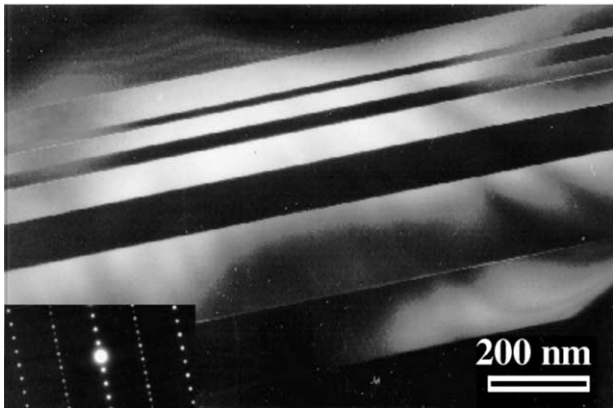

Fig. 4. Dynamical dark field image $\left(\vec{g}=71\bar{1}\right)$ of $Ca_2Nb_2O_7$ near the [011] orientation showing (100) domains.

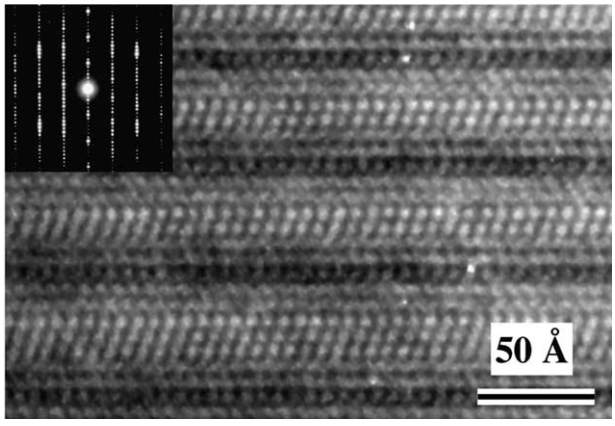

Fig. 5. High-resolution TEM image of $Ca_2Ta_2O_7$. The beam direction is $[110]_{monoclinic}$.

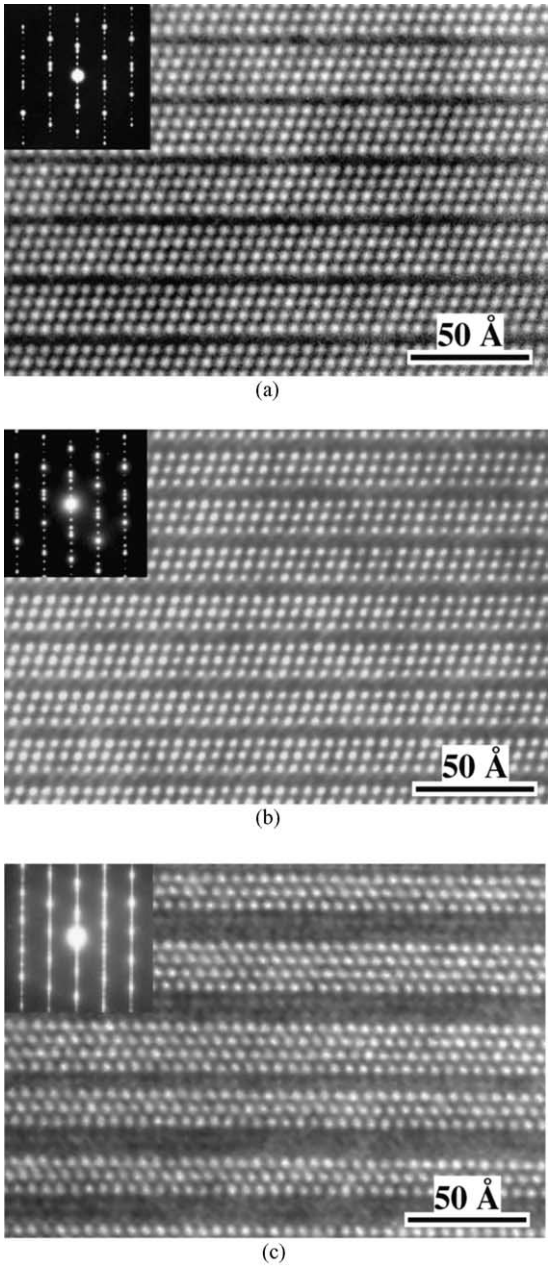

Fig. 6. High-resolution TEM images of grains from ceramics with the nominal compositions (a) $Pb_2Nb_2O_7$, (b) $Pb_2(Nb_{0.5}Ta_{1.5})O_7$, and (c) $(Pb_{0.6}Ca_{1.4})(Nb_{0.5}Ta_{1.5})O_7$. The beam direction is $[100]_{trigonal}$ in each case.

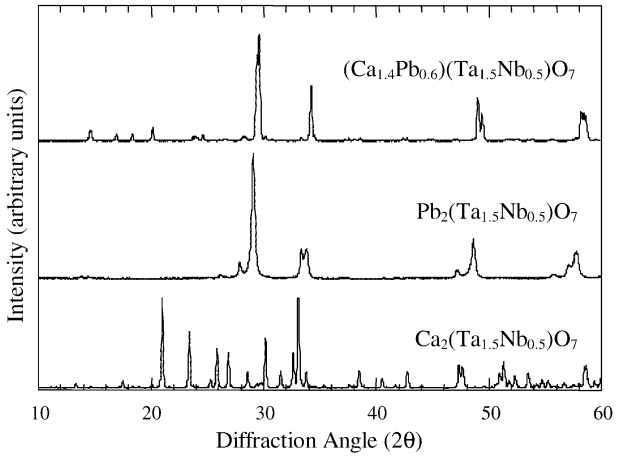

Fig. 7. XRD results for $Pb_2(Ta_{1.5}Nb_{0.5})O_7$, $Ca_2(Ta_{1.5}Nb_{0.5})O_7$ and $(Ca_{1.4}Pb_{0.6})(Ta_{1.5}Nb_{0.5})O_7$.

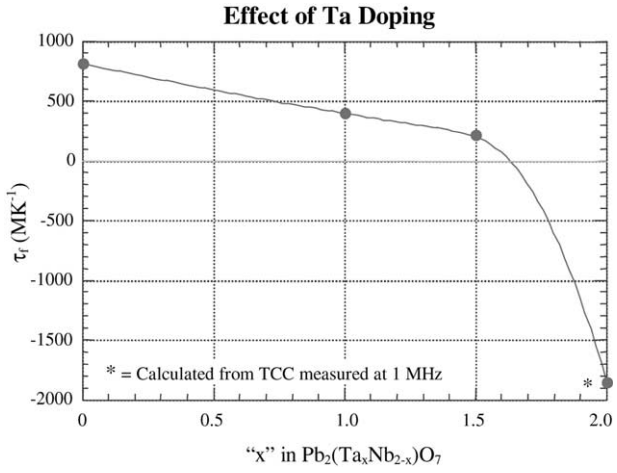

Fig. 8. The variation in τ_f with Ta-content in $Pb_2(Nb_{1-x}Ta_x)_2O_7$. The datum at $x=2$ was calculated from the temperature coefficient of capacitance (TCC) at 1 MHz.

3.2. Microwave properties

The relationship between τ_f and Ta-content is shown in Fig. 8. The lowest $|\tau_f|$ so far achieved is 223 MK^{-1} for $Pb_2(Nb_{0.5}Ta_{1.5})O_7$. Preliminary low-frequency tests have indicated that $Pb_2Ta_2O_7$ may have a τ_f as low as -1855 MK^{-1}, although no resonance was observed in these samples. Similarly, Ca-doping lowered τ_f, but disastrously reduced both Q and ε_r.

4. Conclusions

Cubic $Pb_{1.5}Nb_2O_{6.5}$ has the pyrochlore structure. For higher concentrations of Pb, defect layers appear which destroy the cubic symmetry and reduce it to trigonal. The structure of $Pb_2Nb_2O_7$ is largely unaffected by Ta-doping, but the τ_f is greatly reduced. Replacing some Pb with Ca drastically alters the structure and greatly reduces both Q and ε_r.

Acknowledgements

Electrical measurements were made courtesy of Dr. D. Iddles and Mr. T. Price of Filtronic Comtek, Ceramics Division, Wolverhampton, UK. In addition, the authors are grateful to Dr. Mohamed Bououdina of the University of Nottingham and Dr. Bachir Ouladdiaf of ILL for their help in analysing the neutron diffraction data.

References

1. Ubic, R. and Reaney, I. M., Electron microscopy of lead pyroniobate. *J. Eur. Ceram. Soc.*, 2001, **21**, 2123–2126.
2. Ubic, R. and Reaney, I. M., Microwave properties of doped lead pyroniobate. *J. Eur. Ceram. Soc.*, 2001, **21**, 2659–2662.
3. Ubic, R., Merry, J. C., Leach, A. C. and Reaney, I. M., Defect structure of lead pyroniobates. *Inst. Phys. Conf. Ser.*, 2001, **168**, 19–22.
4. Brusset, H., Mahe, R. and Aung Kyi, U., Caractérisation et comparaison structurales de niobates de type pyrochlore. *C. R. Acad. Sci. C.*, 1972, **C275**, 327–330.
5. Bernotat-Wulf, H. and Hoffmann, W., Die Kristallstrukturen der Bleiniobate vom Pyrochlor-Typ. *Z. Kristallogr*, 1982, **158**, 101–117.
6. Leroux, Ch., Tatarenko, H. and Nihoul, G., High-resolution electron microscopy and modelling of homologous series in non-stoichiometric lead-niobium oxides. *Phys. Rev. B: Condens. Matter*, 1996, **53**(18), 11993–12005.
7. Ubic, R. and Reaney, I. M., Lead niobate ceramics for microwave dielectric resonators. In *Electronic Ceramic Materials and Devices, Vol. 106*, ed. K. M. Nair and A. S. Bhalla. American Ceramic Society, Westerville, OH, 2000, pp. 263–275.
8. Beech, F., Jordan, W. M., Catlow, C. R., Santoro, A. and Steele, B. C. H., Neutron powder diffraction structure and electrical properties of the defect pyrochlores $Pb_{1.5}M_2O_{6.5}$ (M = Nb, Ta). *J. Solid State Chem.*, 1988, **77**, 322–335.
9. Wakiya, N., Saiki, A., Ishizawa, N., Shinozaki, K. and Mizutani, N., Crystal growth, crystal structure and chemical composition of a pyrochlore type compound in lead-magnesium-niobium-oxygen system. *Mater. Res. Bull*, 1992, **28**, 137–143.
10. Ubic, R. and Reaney, I. M., Crystal structure of lead pyroniobate. *Inst. Phys. Conf. Ser.*, 1999, **161**, 157–160.
11. Turner, R. C., Fuierer, P. A., Newnham, R. E. and Shrout, T. R., Materials for high temperature acoustic and vibration sensors: a review. *Appl. Accoustics*, 1994, **41**, 299–324.
12. Grey, I. E., Roth, R. S., Mumme, G., Bendersky, L. A. and Minor, D., Crystal chemistry of new calcium tantalate dielectric materials. *MRS Symp. Proc.*, 1999, **547**, 127–138.